参赛队员姓名： 定浩宸，王佳萱，张智禹

中学： 南京外国语学校

省份： 江苏省

国家/地区： 中国/南部赛区

指导教师姓名： 陈韵聪，许亮亮

指导教师单位： 南京大学，南京外国语学校

论文题目：硒代亚甲基蓝的合成及其 I/II 型光动力治疗的应用

硒代亚甲基蓝的合成及其 I/II 型光动力治疗的应用

定浩宸，王佳萱，张智禹

南京外国语学校，江苏，210018

摘要： 光动力疗法（PDT）由于其非侵入性、高选择性和低毒副作用等优点，正在成为治疗肿瘤的重要手段，然而传统的光敏剂往往受限于治疗窗口短、光漂白性严重、暗毒性大和依赖氧气等缺点，难以进一步应用。本研究将商业化光敏剂亚甲基蓝（MB）进行单原子改造设计，合成了新型光敏分子硒代亚甲基蓝（MBSe），并探究了其对癌细胞和拟肿瘤组织中的治疗效果。实验结果表明硒原子的引入延长了亚甲基蓝光敏剂的最大吸收/发射波长，基于重原子效应提高了光敏剂分子的单重态氧产率，还极大地增强了其 I 型光动力效应。细胞实验结果表明 MBSe 光敏剂在常氧和乏氧条件下均能有效杀死肿瘤细胞，这对于新型光敏剂研发以及 PDT 在肿瘤治疗中的应用具有重要意义。

关键词： 亚甲基蓝，光敏剂，光动力治疗，肿瘤微环境。

Synthesis of Selenomethylene Blue and its Application in Type I / II Photodynamic Therapy

Ding Haochen, Wang Jiaxuan, Zhang Zhiyu

Nanjing Foreign Language School, Jiangsu Province, 210018

Abstract: Being highly selective, non-intrusive, and minimally toxic, photodynamic therapy (PDT) is becoming a critical approach in cancer treatment. However, further implementation of traditional photosensitizers is limited due to drawbacks including short treatment windows, severe photobleaching, dependent on oxygen, etc. In this research, we made a monoatomic modification on a commercialized photosensitizer, Methylene Blue (MB), and synthesized a novel photosensitive molecule Selenomethylene Blue (MBSe). We then studied their therapeutic effects on cancer cells and simulated tumor organisms. The results showed that the introduction of the Selenium atom has extended the maximum absorption/emission wavelength, increased singlet oxygen yield, and significantly enhanced its Type I PDT effect. The cell experiments showed that MBSe can effectively kill cancer cells both in normoxic and hypoxic conditions. This is important for the development of novel photosensitizers and the implementation of PDT in cancer treatment.

Key words: methylene blue, photosensitizer, photodynamic treatment, tumor microenvironment

Catalogue

1 Introduction

1.1 Research Background

Cancer is among the major causes of human death. According to the International Agency for Research on Cancer (IARC), cancer caused 9.7~10.2 million deaths in 2020. Current treatments for cancer are mainly surgical resection, radiotherapy, and chemotherapy. However, traditional cancer treatments have little selectivity and apparent side effects. Cytotoxic medicines would damage normal cells as they kill tumor cells, causing a range of problems including organism necrosis, digestion and immune system disorders, etc. A novel anti-tumor approach, photodynamic therapy (PDT), which is non-intrusive, and highly selective with relatively few side effects, overcomes the drawbacks of traditional cancer treatments.

1.2 PDT Mechanisms

In PDT, the photosensitive molecules that concentrate at tumor sites are excited by a laser of a specific wavelength. Excited photosensitizers then interact with O_2 and generate cytotoxic reactive oxygen species (ROS) after a series of photochemical reactions to kill the cancer cells. Light source, photosensitizer, and oxygen are the three critical factors influencing the PDT effect. Under laser irradiation, the photosensitizers absorb photons and are excited to the excited singlet state.

The photosensitizers at the excited singlet state can return to the ground state by releasing fluorescence or transit to the excited triplet state, which has lower energy, by inter-system crossing. The triplet photosensitizers can (1) transfer electrons or photons to certain substrates to generate radicals or negative ions, which would further react with oxygen to produce cytotoxic ROS (Type I PDT), or (2) directly transfer energy to oxygen molecules, generating reactive singlet oxygen (Type II PDT). ROS produced would further induce apoptosis or necrosis in tumor cells.

1.3 Light Source

The wavelengths of the laser used in PDT usually lie between 600~900 nm. Endogenous molecules in human bodies such as hemoglobin usually have considerable absorption below 600 nm. This would disrupt the photosensitizers' absorption of lasers with similar wavelengths. On the other hand, lasers with wavelengths above 900 nm have relatively low energy, which may result in compromised singlet quantum yield.

1.4 Photosensitizers

An ideal PDT photosensitizer should have high triplet quantum yields, strong light absorption at translucent areas of the organism, and the ability to target tumor

cells. In order not to damage normal tissue, the dark toxicity of photosensitizers should remain low alongside sufficient phototoxicity. The first-generation PDT photosensitizers are mainly porphyrin compounds and their derivatives. While widely admitted for clinical treatments, they have problems of short excite wavelengths, insufficient selectivity, excessive side effects, etc. The second generation are mainly composed of porphyrin derivatives, phthalocyanine and naphthalocyanine compounds, non-porphyrin phenothiazine dyes, and thick ring quinone compounds. They have longer absorption wavelengths and higher cytotoxic species quantum yields compared to their predecessors. The focus of this research, MB, is classified as a second-generation phenothiazine photosensitizer. Now a widely used commercial dye, MB is among the photosensitizers earliest used in clinical antibacterial research. Data show that it effectively inhibits development of cancer organisms such as colon tumors under red light irradiation.

1.5 Oxygen

While Type II PDT may possess higher ROS yield due to lower energy demand for generating singlet oxygen, the extremely low oxygen concentration inside tumors limits the generation. Meanwhile, in Type I PDT, species such as negative ions and radicals generated by the interaction of excited triplet state photosensitive molecules and substrates are able to react with low concentrations of oxygen, generating superoxide anions and ROS such as hydroxyl radicals through reactions including Fenton reaction, Haber-Weiss reaction, etc. As a result, a considerable rate of ROS generation can be maintained through Type I PDT even under the hypoxia conditions inside tumors.

Haber-Weiss Reaction: $O_2^{\cdot-} + H_2O_2 \rightarrow OH^- + O_2 + {}^{\cdot}OH$

Fenton Reaction[3]: $O_2^{\cdot-} + Fe^{3+} \rightarrow O_2 + Fe^{2+}$

1.6 Research Purpose and Methods

PDT's non-intrusiveness, high selectiveness, and low side effects endow it with a promising future for implementation in cancer treatment. The limitations of traditional photosensitizers, namely low ROS yield and heavy dependence on oxygen, provided us with inspiration for new photosensitizer design. We devised the novel photosensitive molecule Selenomethylene Blue (MBSe) by substituting the sulfur atom in the commercialized dye MB with a selenium atom. The high nuclear charge of the selenium atom enhances the spin-orbit coupling of the photosensitizer molecule, thus increasing the rate of inter-system crossing between the singlet and triplet states, which in turn elevates the ROS generation efficiency of the photosensitizer, resulting in stronger anti-tumor properties [15]. In our work, we synthesized MBSe, examined its optical properties, light/dark cytotoxicity under normoxic/hypoxic conditions, and ROS yields, and conducted comparative tests of MBSe and MB, which proved that MBSe has a great potential for application in antitumor therapy.

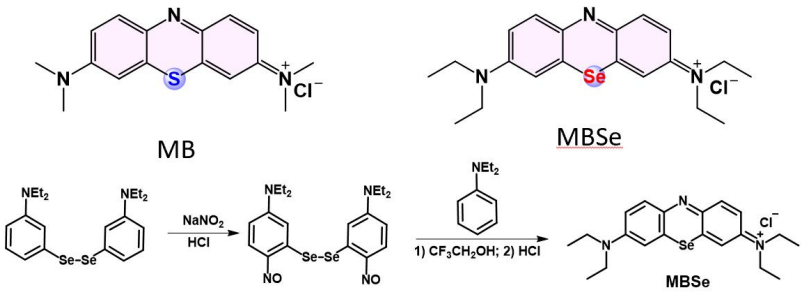

Figure 1.6.1 Structural comparison of MB and MBSe and the synthesis route of the target compound MBSe

2. Materials and Methods

2.1 Materials and Reagents

The commercial dye MB and reagents used for the MBSe preparation were of analytical grade and were purchased from Energy Chemistry and J & K Chemical. The DCFH-DA probes and DHE probes for the detection of ROS and superoxide anion concentrations and the Calcein AM and PI kit for live/dead cells assay were purchased from Beyotime Biotechnology.

2.2 Instruments

We detected fluorescence quantum yield using a Horiba FluoroMax-4 fluorescence spectrophotometer (Horiba Corporation, Japan); we recorded the absorption spectrum and detected the molar absorption coefficient using Perkin Elmer E35 UV-Vis spectrophotometer (Platinum Elmer, USA); we performed cell confocal imaging using a Zeiss LSM710 fluorescence microscope (Zeiss Group, Germany).

2.3 Methods

2.3.1 Synthesis and Structural Characterization of MBSe

3 g (6.6 mmol) double- (3-N, N-diethyl-benzene group) disele was dissolved in 60 mL 1 M hydrochloric acid and placed in an ice water bath. 0.91 g (13.2 mmol) $NaNO_2$ were dissolved in 15 mL of water, slowly dropped into the reaction system in the ice water bath, and stirred constantly. Brick red products were obtained after 10 min of reaction. The reaction solution was extracted with dichloromethane (2*100 mL). The organic phase was dried with anhydrous sodium sulfate, then filtered to get the brick red filtrate, which was concentrated in a rotary evaporator. After adding 3.2 g (21.5 mmol) N, N-diethyl-aniline and dissolving it in trifluoroethanol, we heated it to 90 degrees Celsius, stirring, and obtained a dark blue solution after 1 h of reaction. The solution was concentrated using a rotary evaporator and then purified with a silica gel column with dichloromethane/ethanol (v:v=19:1) as eluent, leaving blue-

black products. The products were characterized by ^{1}H NMR and ^{13}C NMR spectra. The characterization results are listed as follows: ^{1}H NMR (400 MHz, MeOD) δ 7.96 (d, J = 9.6 Hz, 1H), 7.62 (d, J = 2.8 Hz, 1H), 7.38 (dd, J = 9.6, 2.8 Hz, 1H), 3.75 (q, J = 7.2 Hz, 4H), 1.37 (t, J = 7.2 Hz, 6H). ^{13}C NMR (101 MHz, MeOD) δ 153.78, 141.64, 138.32, 136.48, 119.41, 110.76, 47.46, 13.23.

2.3.2 Optical Properties Determination

MB and MBSe were prepared into 1*10^{-5} M solutions with methanol as solvent. Absorption and fluorescence spectroscopy were determined using a UV-Vis spectrophotometer and fluorescence spectrophotometer (grating =3, slit width =4 nm, medium voltage). The fluorescence quantum yield of MB versus MBSe was determined using Neil blue as the reference of the fluorescence quantum yield.

Fluorescent Quantum Yield (QY) is determined according to the following equation:

$$\phi_{sample} = \phi_{ICG} \times \frac{I^{sample} A^{ICG}}{I^{ICG} A^{sample}} \times [\frac{\eta^{sample}}{\eta^{ICG}}]^{2}$$

The molar light absorption coefficient is determined according to the following equation:

$$\varepsilon = \frac{A}{b \times c}$$

The wavelength-matched methylene blue (MB) was used as the standard singlet oxygen reference (ΦΔ =0.52); the DPBF was used as the singlet oxygen capture agent; the MBSe singlet oxygen yield was tested with UV-Vis spectrophotometry. We made 1*10^{-5} M MB and MBSe solutions using methanol as solvent. The solutions were irradiated for 10 s using 2 mW/cm, 635 nm laser after adding DPBF.

Spectra were determined using a UV-Vis spectrophotometer. The experiment was repeated for 10 times. The singlet oxygen yield is determined according to the following formula:

$$\phi_{\Delta}(^{1}O_{2})^{MBSe} = \phi_{\Delta}(^{1}O_{2})^{RB} \frac{S^{MBSe} F^{MB}}{S^{MB} F^{MBSe}}$$

We made 1*10^{-5} M MB and MBSe solutions using methanol as solvent. We added 1*10^{-5} M DHR-1,2,3 and measured the spectra with a UV-Vis spectrophotometer after irradiating for 30 s with 10 mW/cm^{2}, 660 nm laser. The experiment was repeated 8 times.

2.3.3 Theoretical Calculations of the Heavy Atom Effect

The following formula is provided for the molecular inter-system crossing rate:

$$SOC = \langle S_n | H_{SO} | T_m \rangle$$

$$K_{ISC} \propto [\langle S_n | H_{SO} | T_m \rangle / \Delta E_{SnTm}]^{2}$$

Through the Gaussian Density Functional Theory calculation (DFT), we obtained the following data:

Table 2.3.3.1. Singlet and triplet energy gaps and spin-orbit coupling constants for MB and MBSe

Energy (eV)	MB	MBSe	〈S_n|H_{SO}|T_m〉（cm^{-1}）	MB	MBSe
S_1	2.320	2.319	S_1↔T_1	0.050	0.308
T_1	1.137	1.131	S_1↔T_2	0.363	2.066
T_2	1.755	1.662	S_1↔T_3	0.233	0.905
T_3	2.600	2.575	S_1↔T_4	1.150	9.387
T_4	2.659	2.571			
ΔE_{S1T1}	1.183	1.188			
ΔE_{S1T2}	0.565	0.657			
ΔE_{S1T3}	-0.280	-0.256			
ΔE_{S1T4}	-0.339	-0.252			

Table 2.3.3.2. Calculation results of MB and MBSe's $[\langle S_n|H_{SO}|T_m\rangle/\Delta E_{SnTm}]^2$

[〈S_n|H_{SO}|T_m〉/ΔE_{SnTm}]^2（$\times 10^6$）	MB	MBSe
S_1↔T_1	0.00	0.010
S_1↔T_2	0.064	1.527
S_1↔T_3	0.107	1.930
S_1↔T_4	1.776	214.179
Sum	1.947	217.646

（The calculation results of $[\langle S_n|H_{SO}|T_m\rangle/\Delta E_{SnTm}]^2$ do not contain units)

2.3.4 Intracellular ROS Levels and Superoxide Anion Levels Determination

4T1 mouse breast cancer cells (hereinafter referred to as "4T1 cancer cells") were cultured in an incubator after resuscitation with a modified Eagle medium (DMEM, Gibco), which contained 10% FBS (FBS; Gibco) and glutamine (2 mM), under 5% CO_2, saturated humidity, 37℃. Cells in the logarithmic growth phase were seeded in a 30 mm four-grid confocal plate and cultured until a layer of cells at the bottom of the plate appeared. 500 μL of culture medium was added in the four grids, including: 1 μM MB + 5 μM DCFH-DA; 1 μM MB + 5 μM DHE; 1 μM MBSe + 5 μM DCFH-DA; 1 μM MBSe + 5 μM DHE. After 1 h of incubation, the cells were washed three times with PBS and irradiated with 15 mW/cm^2, 635 nm laser for 5 min. After irradiation, they were observed with a fluorescence microscope, excited at 488 nm to detect the fluorescence effect of DCF from 498 nm to 580 nm. They were excited at 488 nm and observed with a 63x oil microscope to detect the fluorescence effect of DHE from 550~680 nm.

In addition, another four-grid confocal plate was used as a control group to detect the intracellular ROS level and the superoxide anion level in the dark environment. Irradiation was skipped, while the other operations were the same.

Two four-grid confocal plates were used as the hypoxic control group to detect

the intracellular ROS and superoxide anion levels under hypoxic conditions. After inoculation of cells and drugs, they were loaded into a hypoxic bag with an anaeropouch peace tablet to simulate the hypoxic environment. Other operations were the same.

2.3.5 Live/Dead Cells Assay

4T1 cancer cells were cultured in an incubator after resuscitation with a modified Eagle medium (DMEM, Gibco) containing 10% FBS (FBS; Gibco) and glutamine (2 mM) under 5% CO_2, saturated humidity, 37°C. Cells in the logarithmic growth phase were seeded in two 30 mm plates and cultured until a layer of cells at the bottom of the plates appeared. Both plates were supplemented with 1.5 mL of 0.5 μM MB and 1.5 mL of 0.5 μM MBSe of strip culture medium and incubated for approximately 1 h. Then, they were irradiated by a 15 mW/cm^2, 635 nm laser for 20 min. 7 mL medicated medium was then prepared with 10 μL Calcein AM and 7 uL PI. After aspirating the original medium, the plates were added with medicated medium and stained for 30 min. They were excited at 490 nm and observed with a fluorescence microscope at 40x to detect the fluorescence strength of the cells at 545nm wavelength.

Two 30 mm plates were taken as the hypoxic control group, performing live/dead cells detection under hypoxic conditions. After inoculation of cells and drugs, they were loaded into a hypoxic bag with an anaeropouch peace tablet to simulate the hypoxic environment. Other operations were the same.

2.3.6 Photosensitizer Cytotoxicity Determination

4T1 cancer cells were cultured in an incubator after resuscitation with a modified Eagle medium (DMEM, Gibco) containing 10% FBS (FBS; Gibco) and glutamine (2 mM) under 5% CO_2, saturated humidity, 37°C. Cells from the logarithmic growth phase were seeded in 96-well plates, whose outermost circle wells were filled with FBS serum. We then seeded the cells in the internal 6*10 wells and cultured them for 24 h until approximately 4500~5000 cells per well appeared. The produced MBSe was prepared into a 10 mM concentrated storage solution. 1.2 μL MBSe concentrated solution was added into DMEM incomplete high glucose medium, making 6 mL of 2 μM MBSe solution. Then, we added 200 μL MBSe solution to the seeded wells, whose concentrations were 2, 1, 0.5, 0.25, 0.125, 0.0625 ,0.0.0313, 0.0156, 0.0.078, and 0.0039 μM respectively from right to left. The far right was 2 μM, decreasing from right to left with a common ratio of 0.5. They were diluted and added with the MB/MBSe solutions we prepared. After 24 h of culture in darkness, 40 μL 2.5 mg/mL MTT solution was added to each well. Cells in the wells were cultured in darkness for 3~4 h after the MTT solution was added. After irradiating them with 15 mW/cm^2, 635 nm laser for 5 min, we carefully aspirated the medium and added 100 μL DMSO to each well to dissolve the blue crystals. Solution absorbance was measured using an enzyme-linked immunodetector. The experiment was repeated. Mean absorbance

percentage and standard deviation of the dosing group were calculated using the absorbance data of the 3 groups obtained in the experiment under the assumption that the absorbance of the group unmedicated was 1. The value of MBSe IC_{50} was then calculated.

Another plate with cells was put into a bag with an anaeropouch tablet after the MB/MBSe solution was added to simulate the hypoxia environment. Other operations were the same.

For dark toxicity detection, no irradiation was required. 76.8 uL of 10 mM MBSe concentrated storage liquid was added to incomplete high glucose medium, making 6 mL of 128 μM MBSe solution. 200 μL MBSe was added in the 96-well plates, with concentrations of 128, 64, 32, 16, 8, 4, 2, 1, 0.5, and 0.25 μM respectively from right to left. Other operations were the same.

MB was used for the comparative test, with the same operations. Solution absorbance at 490/570 nm was measured by an enzyme-linked immune detector. The value of MB IC_{50} was calculated. Other operations were the same.

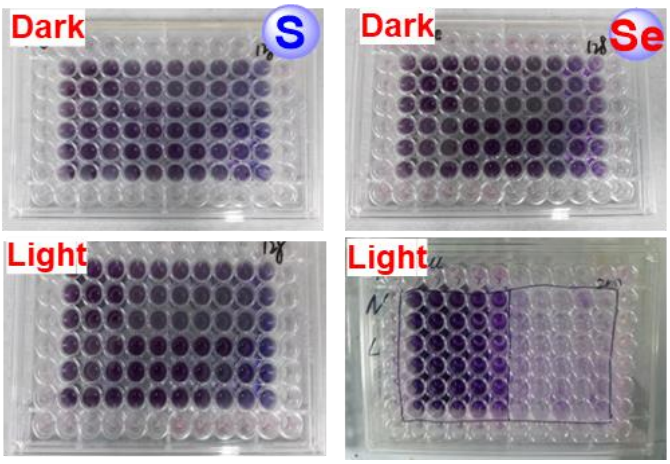

Figure 2.3.6.1 The results of MTT experiment

2.3.7 Simulated Tumor Cell Spheroid Experiment

4T1 cancer cells were cultured in an incubator after resuscitation with a modified Eagle medium (DMEM, Gibco) containing 10% FBS (FBS; Gibco) and glutamine (2 mM) under 5% CO_2, saturated humidity, 37°C. Cells in the logarithmic growth phase were seeded in a 96-well ultra-low adsorption plate with marginal wells filled with sterile PBS, approximately 5,000 cells per well. The cells were cultured for 24h until they covered the bottom of the plate and formed a spheroid. The 6*10 wells inside were then divided into 10 groups of 3*2 wells from left to right, labeled from 1 to 10, as shown in Figure 2.3.7.1.

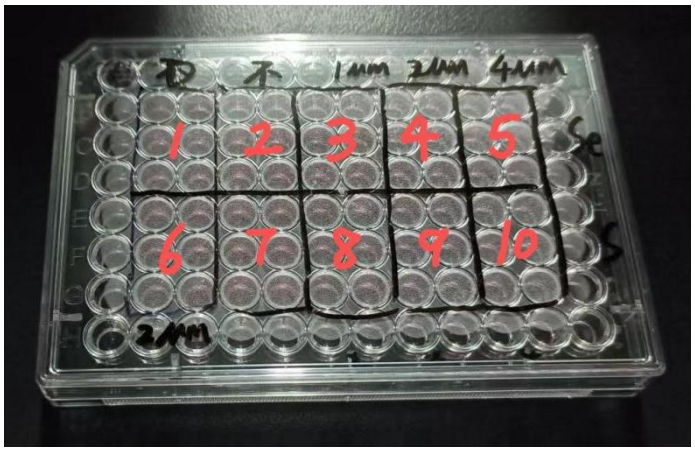

Figure 2.3.7.1 96-well ultra-low adsorption plates for cell spheres culture

The following treatments were applied to each group: 1: add 2 μM MBSe; 2: unmedicated; 3: add 1 μM MBSe; 4: add 2 μM MBSe; 5: add 4 μM MBSe; 6: add 2 μM MB; 7: unmedicated; 8: add 1 μM MB; 9: add 2 μM MB; 10: add 4 μM MB. After 24 h of culture in darkness, groups 2, 3, 4, 5, 7, 8, 9, 10 were exposed to 15 mW/cm^2, 635 nm laser irradiation for 5 min. We performed confocal imaging with a fluorescence microscope, then cultured the cells in darkness for 24 h and did the imaging once more.

3 Results and discussion

3.1 Structural Characterization of MBSe

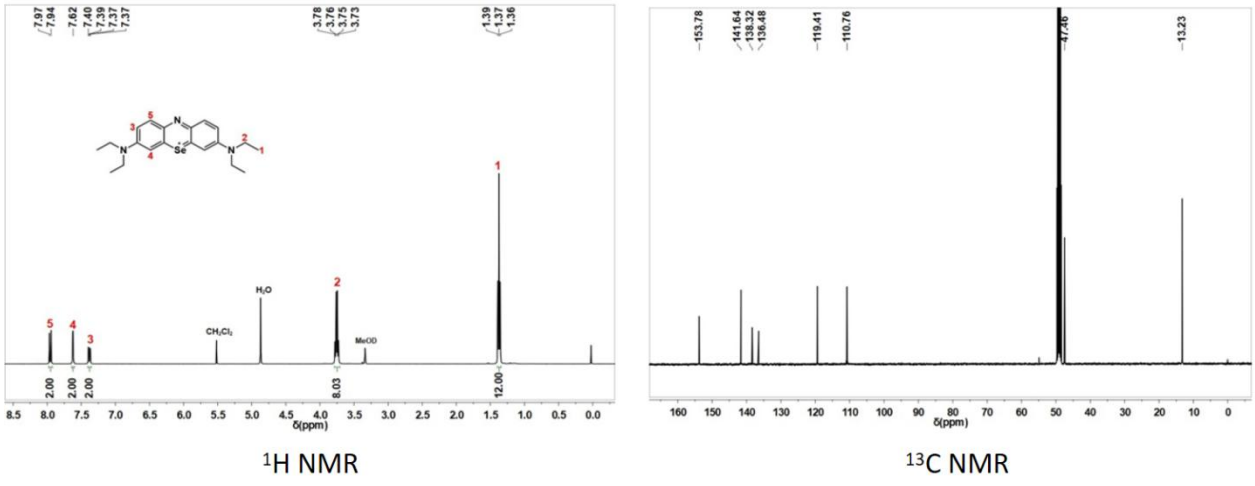

Figure 3.1.1 NMR hydrogen spectrum / carbon spectrum structural characterization of MBSe

In the ^{1}H NMR spectrum, six proton chemical shifts appeared at 7.38~7.97 ppm, corresponding to six protons on the acridine ring; eight at 3.75~3.78 ppm, corresponding to eight protons on four methylene groups; and twelve at 1.36~1.39 ppm, corresponding to twelve protons on four methyl groups. In the ^{13}C NMR

spectrum of MBSe, acridine ring carbon signals appeared at-110.76~-155.78 ppm, and methyl and methylene carbon signals appeared at -13.23~-47.46 ppm. The structural characterization above indicated the successful synthesis of the MBSe molecule.

3.2 Optical Properties of MBSe

We measured the absorption and fluorescence spectra of MB and MBSe with UV-Vis spectrophotometer and fluorescence spectrophotometer and measured the fluorescence quantum yields of MB and MBSe using Nel blue as the reference. We also measured the singlet oxygen yield of MBSe using DPBF as singlet oxygen trapping agent and MB as the reference. Moreover, we measured the relative yields of MB and superoxide anions of MBSe using DHR-1,2,3 as the capture agent of superoxide anions. DPBF has a fluorescence effect with a maximum wavelength of 455 nm under 410 nm laser excitation, and it is easy to react with singlet oxygen to produce oxidation products with small absorbance at 410 nm and no fluorescence effect. The yield of the generated singlet oxygen can be determined by detecting the change of the solution's light absorption at 410 nm [17]; DHR-1,2,3 itself does not have a fluorescence effect and can be oxidized to R-1,2,3 by superoxide anions. R-1,2,3 will accumulate in intracellular mitochondria and emit green fluorescence. The superoxide anion yield can be determined by detecting the intracellular fluorescence intensity changes[18]。

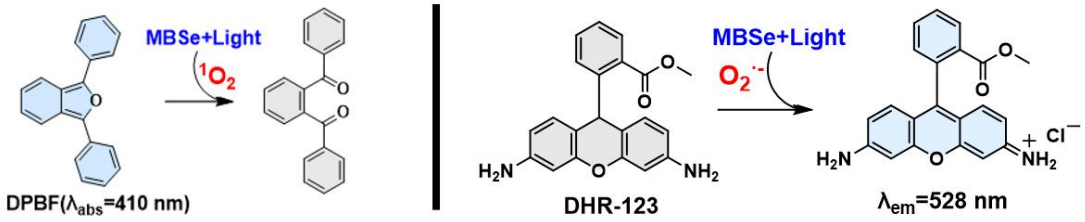

Figure 3.2.1 Principles of DPBF and DHR-1,2,3 detection

The results of the spectral experiments are shown in Figure 3.2.2.

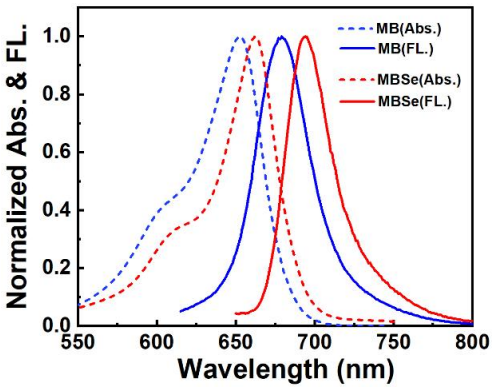

Figure 3.2.2 The absorption and fluorescence emission spectra of MB and MBSe

Compound	λ_{abs}/ nm	$\varepsilon/10^4$ $M^{-1}cm^{-1}$	λ_{em}/nm	Stokes Shifts (nm)	Φ_f	Φ_Δ
MB	652	8.34	680	28	0.23	0.52
MBSe	662	12.26	695	33	0.03	0.81

Figure 3.2.3 The data analysis of spectra of MB and MBSe

The detection results of singlet oxide and superoxide anion yield are shown in the figures below:

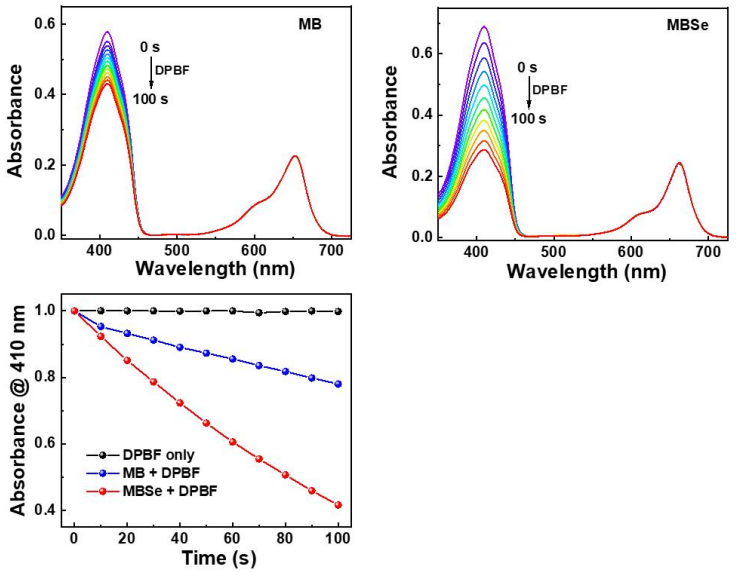

Figure 3.2.4 The UV-Vis spectra of the DPBF fluorescence probe measuring singlet oxygen yield (2 mW/cm^2, 10 s)

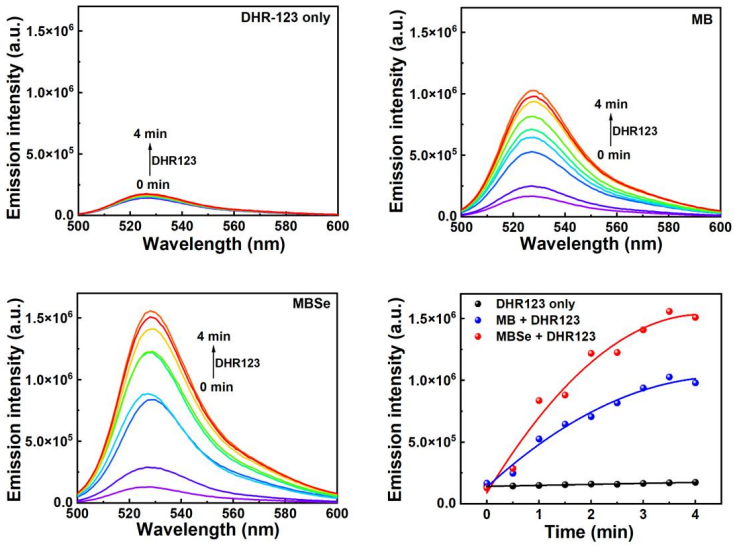

Figure 3.2.5 The UV-Vis spectra of DHR-1,2,3 probe detecting relative yield of superoxide anions (10 mW/cm^2, 30 s)

As can be seen from Figure 3.2.3, the maximum absorption wavelength of MB is 652 nm, with a fluorescence emission wavelength of 680 nm and a molar light absorption coefficient of $8.34*10^4$ $M^{-1}cm^{-1}$; The maximum absorption wavelength of MBSe is 662 nm, with a fluorescence emission wavelength of 695 nm and a molar absorption coefficient of $12.26*10^4$ $M^{-1}cm^{-1}$. The above data indicate that the absorption wavelength of MBSe redshifts towards the near-infrared region, and has a better light absorption efficiency within biological tissues. As can be seen from Figure 3.2.4, both MB and MBSe can produce singlet oxygen after irradiation, meanwhile, the DPBF absorption peak of 410 nm drops rapidly. According to the formula, we can calculate the singlet oxygen of the material MBSe in methanol, getting a yield of 0.81, which is higher than the singlet oxygen quantum yield of 0.52 of the commercial dye MB. This shows that MBSe has a better Type II PDT effect compared with MB, mainly because of the heavy atom effect of selenium atoms that promotes inter-system crossing. Such a high singlet oxygen yield ensures that MBSe can be effective in photodynamic therapy. As shown in Figure 3.2.5, the detection of fluorescence intensity changes in DHR-1,2,3 indicates that MBSe is also able to produce more superoxide anions than MB. Its excellent Type I PDT performance enables its better adaptation to intra-tumor hypoxia environment. In conclusion, MBSe simultaneously has both better Type I / II PDT photosensitizer effects in vitro compared with MB. Its properties are worth further exploration.

3.3 Theoretical Calculations of the Heavy Atom Effect

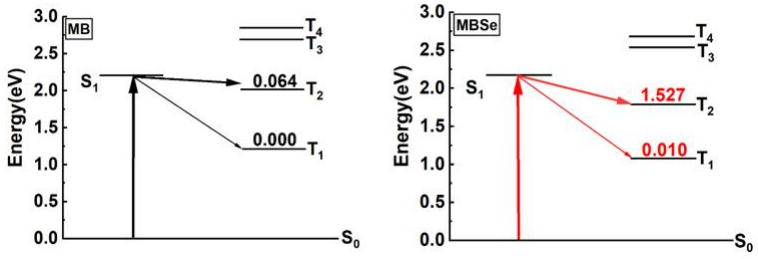

Figure 3.3.1 Comparison of the inter-system crossing rate between MB and MBSe

Through theoretical calculations, we found that after replacing sulfur with selenium, a heavy atom, the SOC constant of MBSe increased significantly and the singlet and triplet energy gap (ΔE_{ST}) changed slightly, leading to a vast increase in inter-system crossing rate (ISC) constant K_{ISC} （$\propto[\langle S_n|H_{SO}|T_m\rangle/\Delta E_{SnTm}]^2$） (see Table 2.3.2.1~2.3.2.2). According to the oscillation strength (f_{OSC}), we discovered that the inter-system crossing from the S1 state to the T2 state was the major contributor to the formation of triplet photosensitizers (f_{OSC}=0.8788). The constant K_{ISC} for MBSe is about 24 times that of MB, very likely indicating better photosensitivity. The results above shows that the introduction of Se atoms endowed MBSe with remarkable potential as a photosensitive reagent.

3.4 Intracellular ROS and Superoxide Anion Levels Determination

We tested intracellular ROS levels using DCFH-DA probe. DCFH-DA probe is not fluorescent itself. After entering the cell, it is hydrolyzed by esterase and forms DCFH, which cannot pass through the cell membrane. DCFH can be oxidized by ROS into DCF, which has light-green fluorescence. Therefore, intracellular ROS levels can be indicated by the fluorescent intensity. We also tested superoxide anion levels using DHE probe. DHE probe can be oxidized by superoxide anions, producing ethidium. The product emits a red fluorescence when combined with the nuclear DNA and RNA. Therefore, superoxide anion levels can be indicated by the fluorescence intensity we measured.

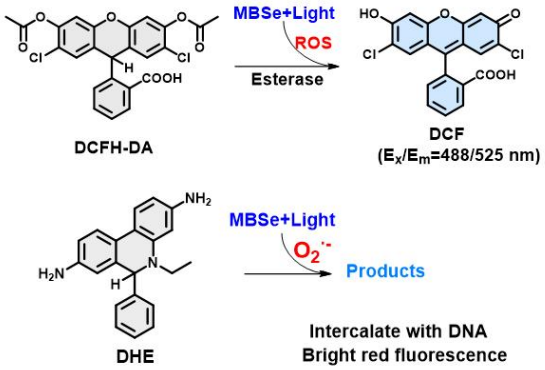

Figure 3.4.1 Molecular structure and detection principle of the small-molecule fluorescent probes DCFH-DA and DHE

The results of intracellular ROS levels test are as below:

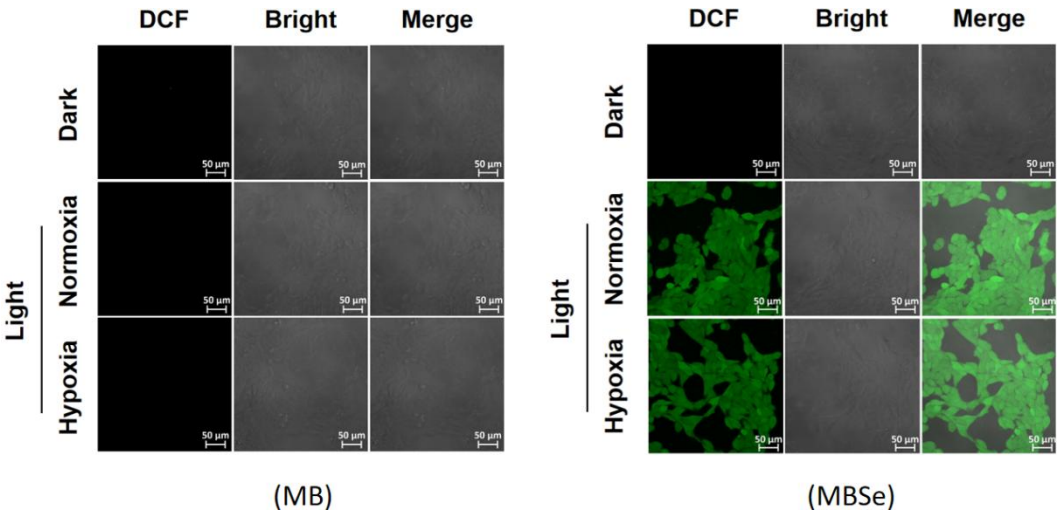

Figure 3.4.2 Confocal imaging of intracellular ROS levels detected in MB and MBSe

As can be seen from Figure 3.4.2, there was no notable fluorescence in the cells cultured in 1 μM MB and 1 μM MBSe under dark conditions. This indicates that

without light, the intracellular ROS levels are low and that neither MB nor MBSe has evident dark toxicity. After 5 min of 15 mW/cm^2, 635 nm laser irradiation, there was still no noticeable fluorescence in 1 μM MB cultured cells, but 1 μM MBSe cultured cells exhibited obvious green fluorescence both in anaerobic and anaerobic conditions. This suggests higher DCF concentration in MBSe cultured cells after irradiation. Thus, compared with MB, MBSe has stronger ROS production ability under laser irradiation and stronger phototoxicity and anti-tumor efficacy. MBSe can still maintain a high ROS production rate under hypoxic conditions, indicating that MBSe has a stronger ability to adapt to the hypoxic environment in tumor tissues.

The results of intracellular superoxide anion levels are as below:

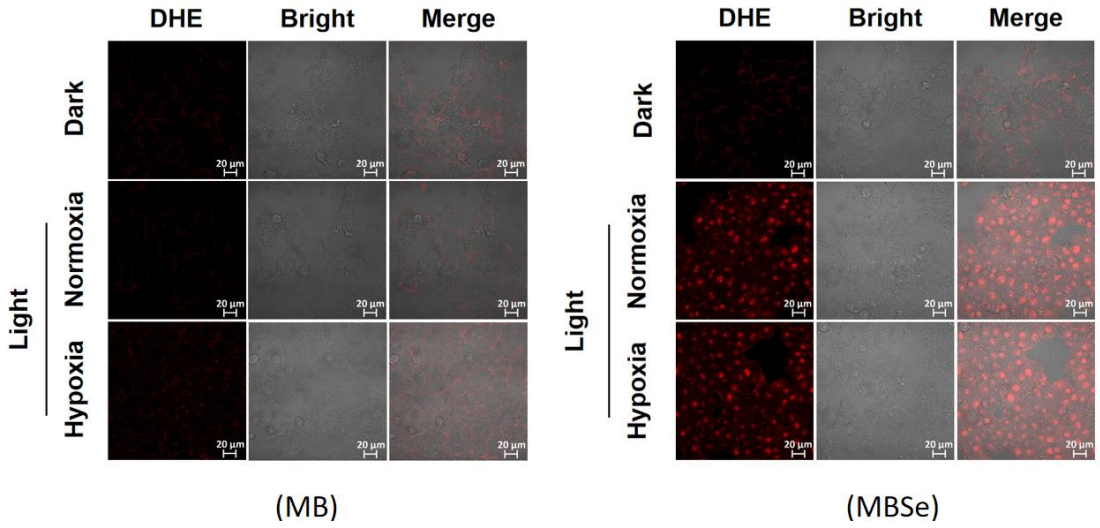

Figure 3.4.3 Confocal imaging of intracellular superoxide anion levels detected in MB and MBSe

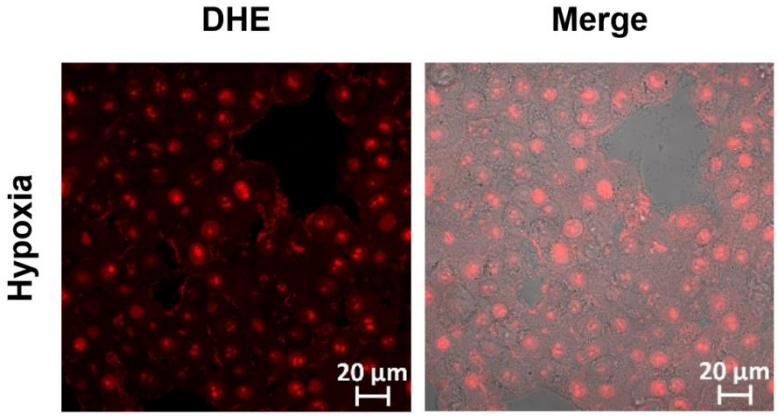

Figure 3.4.4 Confocal imaging of DHE fluorescence probe detection in MBSe cultured cells under hypoxia

As can be seen from Figure 3.4.3, no cells cultured in 1 μM MB or 1 μM MBSe showed a significant fluorescence effect in the dark conditions, meaning that the intracellular superoxide anion levels were low in the dark conditions, and neither MB nor MBSe shows any obvious dark toxicity. After being irradiated by 15 mW/cm^2, 635 nm laser for 5 min, cells cultured in 1 μM MB only showed weak red

fluorescence effect, while cells cultured with 1 μM MBSe showed significant red fluorescence effect under both normoxic and hypoxic conditions. This indicates that MBSe cultured cells have a higher concentration of intracellular DHE oxidation products after irradiation, which indicates that MBSe has a stronger ability to generate superoxide anions than MB when irradiated. This indicates that MBSe has a stronger ability to adapt to the hypoxic environment in tumor tissues. The fluorescence intensity of the cell center in Figure 3.4.4 far exceeded the area of the cell edge, because the ethidium species formed after oxidative dehydrogenation of DHE by superoxide anions bind to the DNA/RNA in the nucleus, resulting in the greater fluorescence intensity of the nucleus region.

3.5 Live/Dead Cells Assay

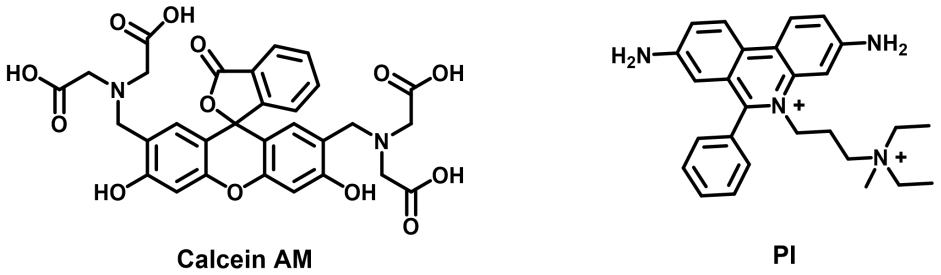

Figure 3.5.1 Molecular structures of the Calcein AM probes and the PI probes

We used Calcein AM/PI probe for live/dead cells assay. Calcein AM can pass through a living cell's membrane. It is hydrolyzed by esterase and produces Calcein, which has a bright green fluorescence and cannot leave the cell. PI (propidium iodide) cannot pass through a living cell's membrane. It only binds with the nuclear DNA in a dead cell and emits a bright red fluorescence. The test results are shown as below:

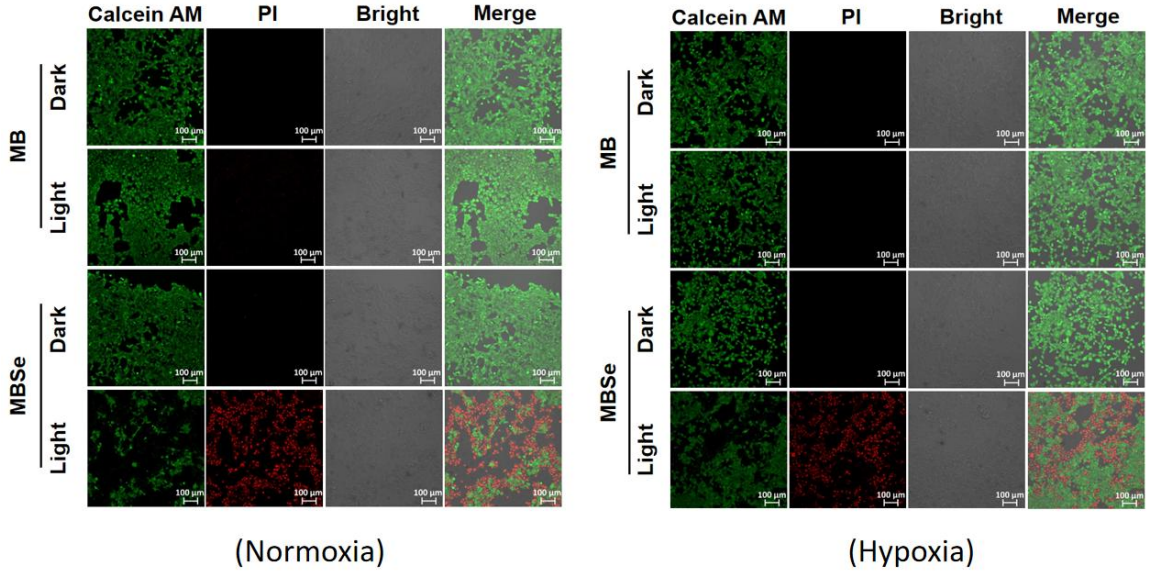

Figure 3.5.2 Confocal imaging of live/dead cells assay results

As can be seen from Figure 3.5.2, after 20 min of 15 mW/cm^2, 635 nm laser

irradiation, the cells cultured in 0.5 μM MB showed obvious green fluorescence but no red fluorescence in both normoxic and hypoxic conditions. However, the 0.5 μM MBSe cultured cells, after the same irradiation, exhibited obvious red fluorescence both in normoxic and hypoxic conditions. This demonstrates the low survival rate of cells cultured in MBSe, indicating MBSe's stronger phototoxicity. Without irradiation, both MB and MBSe cultured cells showed obvious green fluorescence but no red fluorescence, suggesting that neither MB nor MBSe has evident dark toxicity. They both have light-selectivity treatment effects and low side effects.

3.6 Photosensitizer Cytotoxicity Determination

We used methyl thiazole tetrazole (MTT) to determine the dark toxicity and phototoxicity of MB and MBSe on 4T1 cells. Succinate dehydrogenase (SDH), which only exists in a living cell's mitochondria, can reduce MTT to blue-purple methyl crystals. The reduced blue-purple crystals are dissolved in DMSO, and the light absorption value of the solution should reflect the number of primary living cells. The semi-lethal concentration IC_{50} of the photosensitizers can be calculated based on the light absorption values of the unmedicated control group and would reflect the cytotoxicity of the photosensitizer. The experimental results are shown in the following figures.

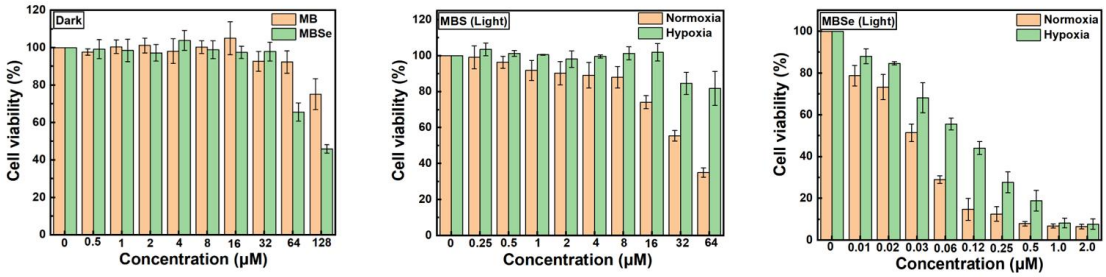

Figure 3.6.1 The viability of cells after growing cells with MB and MBSe at different concentrations and under different conditions

		IC_{50} (μM)	
		Dark	Light
MB	Normoxia	>128	38.66
	Hypoxia		>64
MBSe	Normoxia	85.60	0.033
	Hypoxia		0.087

Figure 3.6.2 Semi-lethal concentration of MB, MBSe under different conditions

As shown in Figure 3.6.1, under normoxic conditions, The viability of the cells cultured in 2 μM of MB was nearly 90% after the irradiation of 15 mW/cm^2, 635 nm laser for 5 min. However, the survival rate of the cells cultured in 2 μM MBSe

after the same laser irradiation was less than 10%. This demonstrates the higher phototoxicity of MBSe under normoxic conditions, which may have resulted from the heavy atom effect. Under hypoxic conditions, cells cultured in 64 μM MB still maintained a viability of over 80% after 15 mW/cm^2, 635 nm lasering for 5 min. This indicates that MB's phototoxicity is limited under hypoxic conditions. However, under the same laser irradiation, less than 10% of cells cultured in 1 μM MBSe under hypoxic conditions survived. This indicates that MBSe still has strong phototoxicity under hypoxic conditions, which helps it better adapt to the oxygen-deprived environment inside the tumor. In Figure 3.6.2, comparing the two median inhibition concentrations (IC_{50}), after irradiation, the IC_{50} of MB under normoxic (IC_{50}, 38.66 μM) and hypoxic (IC_{50}， >64 μM) conditions were significantly larger than that of MBSe. Meanwhile, the light IC_{50} of MBSe was very low (IC_{50}, normoxic 0.033 μM, hypoxic 0.087 μM). This suggests that MBSe has stronger phototoxicity and better antitumor capacity than MB. As shown in Figure 3.6.1, neither MB nor MBSe showed significant dark toxicity at concentrations lower than 16 μM, which already far exceeded the doses that would be used in actual treatments. The IC_{50} of MB and MBSe in dark conditions were both considerably high, indicating that they possess low side effects.

3.7 Simulated Cancer Cell Spheroid Experiment

We simulated a cancer microenvironment and tested the cytotoxicity of MB and MBSe in the environment by cultivating 3-dimensional 4T1 cancer cell spheroids.

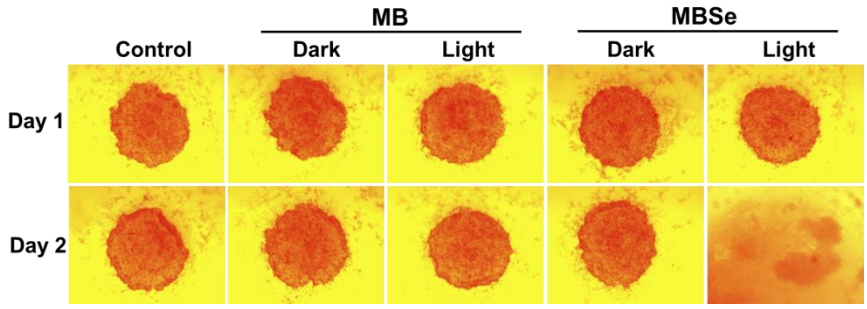

Figure 3.7.1 Confocal imaging of 4T1 cell spheroids cultured under different conditions for 24 h and 48 h

As can be seen in Figure 3.7.1, the cells in the control group showed no significant difference after being cultured for 48 h. No obvious dissociation occurred in the 2 μM MB group, with or without irradiation. This indicates that MB cannot effectively kill cancer cells by generating ROS in the low light and oxygen conditions inside tumors. Meanwhile, the cell spheroids cultured in 2 μM MBSe did not dissociate noticeably in dark, but significantly dissociated and lost clear cell contour after 5 min of 15 mW/cm^2， 635 nm laser irradiation. This shows that MBSe does not have significant side effects in dark and adapts well to inside-tumor conditions. This may be consequent to its stronger capacity of hyperoxide anion generation through Type I PDT.

4 Conclusions

As shown above, based on the heavy atom effect, we introduced a Selenium atom into the commercialized traditional dye MB and devised the photosensitive molecule MBSe, which possesses both type I and II PDT effects. We tested its photophysical properties and cytotoxicity in 4T1 breast cancer cells in a series of spectrum analyses and cell experiments and compared the data with those of MB. By measuring their absorption/emission wavelength range, singlet oxygen quantum production and superoxide anion production, we proved that MBSe has superior in vitro type I and II photodynamic effects. After analyzing the MTT experiment and the results of small-molecule fluorescent probes test in 4T1 cells, we found that MBSe, while maintaining a sufficiently low dark toxicity, has stronger ROS generation capacity than MB. In the stimulated tumor cell spheroid we cultivated, MBSe was found to be more efficient at killing tumor cells under hypoxic environment in tumor tissues. Based on the results listed above, we proved the possibility of designing novel photosensitizers based on the heavy atom effect and successfully devised one with better anti-tumor performance. The traditional MB is already widely used in clinical treatment across the globe. Our improved design should have a broad application prospect.

References

[1] Ferlay J, Ervik M, Lam F, et al.Global cancer observatory: cancer today.Int.Agency Res[J].Cancer, 2020.

[2] W.Fan, B.Yung, P.Huang, X.Chen, Chem.Rev.2017, 117, 13566.

[3] Chen D, Xu Q, Wang W, et al.Type I photosensitizers revitalizing photodynamic oncotherapy[J].Small, 2021, 17(31): 2006742.

[4] Foote C S.Definition of type I and type II photosensitized oxidation[J].Photochemistry and photobiology, 1991, 54(5): 659-659.

[5] Ding H.: Photodynamic therapy: basic principles and applications[M]. Chemical Industry Press, 2014.

[6] Photodynamic therapy[M].Royal Society of Chemistry, 2003.

[7] Robertson C A, Evans D H, Abrahamse H.Photodynamic therapy (PDT): a short review on cellular mechanisms and cancer research applications for PDT[J].Journal of Photochemistry and Photobiology B: Biology, 2009, 96(1): 1-8.

[8] Macdonald I J, Dougherty T J.Basic principles of photodynamic therapy[J].Journal of Porphyrins and Phthalocyanines, 2001, 5(02): 105-129.

[9] Tu Y, Xia W, Wu X, et al.A lysosome-targeted near-infrared photosensitizer for photodynamic therapy and two-photon fluorescence imaging[J].Organic & Biomolecular Chemistry, 2021, 19.

[10] Dai T, Fuchs B B, Coleman J J, et al.Concepts and principles of photodynamic therapy as an alternative antifungal discovery platform[J].Frontiers in microbiology, 2012, 3: 120.

[11] Orth K, Russ D, Beck G, et al.Photochemotherapy of experimental colonic tumours with intra-tumorally applied methylene blue[J].Langenbeck's archives of surgery, 1998, 383(3): 276-281.

[12] Mattila H, Khorobrykh S, Havurinne V, et al.Reactive oxygen species: Reactions and detection from photosynthetic tissues[J].Journal of Photochemistry and Photobiology B: Biology, 2015, 152: 176-214.

[13] Li X, Lee D, Huang J D, et al.Phthalocyanine-assembled nanodots as photosensitizers for highly efficient type I photoreactions in photodynamic therapy[J].Angewandte Chemie International Edition, 2018, 57(31): 9885-9890.

[14] Li M, Xia J, Tian R, et al.Near-infrared light-initiated molecular superoxide radical generator: rejuvenating photodynamic therapy against hypoxic tumors[J].Journal of the American Chemical Society, 2018, 140(44): 14851-14859.

[15] Foley J W, Song X, Demidova T N, et al.Synthesis and properties of benzo [a] phenoxazinium chalcogen analogues as novel broad-spectrum antimicrobial photosensitizers[J].Journal of medicinal chemistry, 2006, 49(17): 5291-5299.

[16] Carloni P, Damiani E, Greci L, et al.On the use of 1, 3-diphenylisobenzofuran (DPBF).Reactions with carbon and oxygen centered radicals in model and natural systems[J].Research on chemical intermediates, 1993, 19(5): 395-405.

[17] LeBel C P, Ischiropoulos H, Bondy S C.Evaluation of the probe 2', 7'-dichlorofluorescin as an indicator of reactive oxygen species formation and oxidative stress[J].Chemical research in toxicology, 1992, 5(2): 227-231.

[18] Kiani-Esfahani A, Tavalaee M, Deemeh M R, et al.DHR123: an alternative probe for assessment of ROS in human spermatozoa[J].Systems biology in reproductive medicine, 2012, 58(3): 168-174.
[19] Jiang X J, Lo P C, Yeung S L, et al.A pH-responsive fluorescence probe and photosensitiser based on a tetraamino silicon (IV) phthalocyanine[J].Chemical communications, 2010, 46(18): 3188-3190.
[20] Zhao H, Joseph J, Fales H M, et al.Detection and characterization of the product of hydroethidine and intracellular superoxide by HPLC and limitations of fluorescence[J].Proceedings of the National Academy of Sciences, 2005, 102(16): 5727-5732.
[21] Qi F, Yuan H, Chen Y, et al.Type I Photoreaction and Photoinduced Ferroptosis by a Ru (II) Complex to Overcome Tumor Hypoxia in Photodynamic Therapy[J].CCS Chemistry, 2022: 1-9.

Acknowledgement

We are three high school students with strong interests in chemistry. We are honored to have the opportunity to get the guidance of teachers, completing the research of anti-tumor therapy and participating in the S.-T. Yau High School Science Award. Along the way, we have been perplexed, but with the solution of one puzzle after another, we have successfully synthesized our ideal photosensitive molecules, completed the scientific research topic, and gained a lot.

On this occasion, we would like to extend our sincerest respect and heartfelt thanks to our tutor, Professor Chen Yuncong, who works at Nanjing University, providing us with careful guidance in topics selection, experimental design, experimental operation, and other aspects. Mr. Chen has rich research experience in the development and application of tumor diagnosis and treatment reagents and keen academic insight. Especially, he is a good role model for us to learn from his tenacity and innovative spirit of exploration in scientific research. In the course of the research, Xu Liangliang, a teacher from Nanjing Foreign Language School, gave us great help and guidance in the theoretical research. Mr. Xu has extensive knowledge, quick thinking, and profound understanding of the academic frontier, and is sincere to others. He is a teacher and also a friend. The two tutors have exerted a profound influence on our school, scientific research, and life. Here we would like to express our sincere gratitude! During our study and research, we received the selfless help and guidance from senior Yao Shankun. Under his guidance, we gained a deeper understanding of the principles of photodynamic therapy, and at the same time, became more skilled in the biochemical experiments involved and had richer laboratory experience. In the process of writing and revising our paper, Senior Yao also provided guidance very patiently. We hereby express our most sincere thanks to him!

The three of us had a clear division of labor. Ding Haochen was responsible for the collection and sorting of literature materials, participated in the design of experimental schemes, and was responsible for the synthesis of photosensitizer molecules and the determination of photophysical properties. Jiaxuan Wang was responsible for live/dead cells assay and simulated tumor cell sphere experiment, and analyzed the feasibility of the detection protocol. Zhang Zhiyu is responsible for photosensitizer cytotoxicity assay, intracellular reactive oxygen species level and superoxide anion level detection. Under the guidance of our instructor and senior student, we completed the theoretical calculation of heavy atom effects and the structure characterization of compounds. Ding Haochen was responsible for writing the first draft of the paper, Wang Jiaxuan was responsible for data collation and mapping, and Zhang Zhiyu was responsible for literature collation. All three of us participated in the revision of the article.